Electronic structure and bonding in epitaxially stabilized cubic iron silicides

Kurt A. Mäder* and Hans von Känel

Laboratorium für Festkörperphysik, Eidgenössische Technische Hochschule Hönggerberg, CH-8093 Zürich, Switzerland

Alfonso Baldereschi†

*Institut Romand de Recherche Numérique en Physique des Matériaux, Ecublens, CH-1015 Lausanne, Switzerland
and Institut de Physique Appliquée, Ecole Polytechnique Fédérale Lausanne, CH-1015 Lausanne, Switzerland*

We present an *ab initio* full-potential linearized augmented-plane-wave (FLAPW) study of the structural and electronic properties of the two bulk unstable compounds FeSi (CsCl structure) and FeSi$_2$ (CaF$_2$ structure) which have recently been grown by molecular-beam epitaxy on Si(111). We obtain equilibrium bulk lattice constants of 2.72 and 5.32 Å for FeSi and FeSi$_2$, respectively. The density of states (DOS) of FeSi agrees well with experiment and shows metallic behavior. In agreement with a previous calculation, the DOS of FeSi$_2$ shows a large density of d states at the Fermi level, explaining the instability of the bulk phase. The electron charge distributions reveal a small charge transfer from Si to Fe atomic spheres in both compounds. While in FeSi the Fe-Si bond is indeed partially ionic, we show that in FeSi$_2$ the electron distribution corresponds to a covalent charge accumulation in the Fe-Si bond region. The reversed order of d bands in FeSi with respect to FeSi$_2$ is understood in terms of crystal-field splitting and Fe-Fe nearest-neighbor dd interactions in the CsCl structure, and a strong Si p–Fe d bonding in the fluorite structure, respectively.

I. INTRODUCTION

The current interest in transition-metal silicides stems from both fundamental and technological issues. For applications in microelectronics and optoelectronics the main focus is on silicides which can be grown epitaxially on Si such as, e.g., NiSi$_2$ and CoSi$_2$ whose small lattice mismatch with Si allows for the synthesis of high-quality semiconductor-metal heterostructures.[1] These systems open the way for the study of intriguing fundamental questions, such as Schottky barrier formation, interface structure, growth kinetics, and stability of novel epitaxial phases. Whereas the CaF$_2$ structure of both CoSi$_2$ and NiSi$_2$ are stable bulk phases of these compounds, FeSi$_2$ does not crystallize in the fluorite form. At this stoichiometry and below $\sim 1000\,°$C its stable bulk form is[2,3] β-FeSi$_2$, which is semiconducting. This orthorhombic structure can be regarded as a distorted fluorite structure, and its greater stability with respect to the fluorite phase can be understood in terms of the electronic structure of the latter: a high density of d states (d DOS) at the Fermi level E_F leads to a Jahn-Teller-like instability of fluorite[4] FeSi$_2$. In β-FeSi$_2$ the d levels are crystal-field split at E_F, and the opening of a gap[4] ($E_g \approx 0.8$ eV) leads to semiconducting behavior. At composition 1:1 in the Fe-Si phase diagram[3] we find the compound ϵ-FeSi. This structure is actually referred to as the "FeSi" structure, and its Pearson symbol is $cP8$.

Under the growth conditions of molecular-beam epitaxy (MBE) on Si(111) the Fe-Si phase diagram is dramatically different:[5–7] at a Fe/Si composition ratio of 1:2 not only epitaxial β-FeSi$_2$ is found, but also the bulk

unstable fluorite phase, denoted γ-FeSi$_2$ in Ref. 6. At composition 1:1 besides ϵ-FeSi the CsCl structure of FeSi grows pseudomorphically on Si(111). Hence we deal with two novel materials completely absent in the bulk phase diagram. Before turning to the electronic and structural properties of these two structures, let us briefly discuss the physical mechanisms pertinent to the occurrence of novel epitaxial phases. (We shall use the term "epitaxial phase" only for novel phases which do not exist in bulk form, in order to emphasize their distinctiveness from stable bulk phases which may also be present in epitaxial phase diagrams.)

We distinguish two classes of epitaxial phases: (i) epitaxially stable phases, where the strain conditions imposed by the substrate select a species with a lower epitaxial formation enthalpy than the strained bulk phase at that particular substrate lattice constant;[8,9] (ii) epitaxially metastable phases, where kinetic barriers inhibit the transformation to a (epitaxially) more stable phase.

For 1:1 FeSi, we argue that up to a critical film thickness the CsCl structure of FeSi belongs to class (i), i.e., it is epitaxially stable on Si(111). Experimentally[7] it is found that low-temperature MBE growth of FeSi on Si(111) yields coherent films in the CsCl structure up to ~ 100 Å, above which the creation of misfit dislocations leads to partial relaxation. Films thicker than 15 Å transform into relaxed ϵ-FeSi upon annealing at $\sim 300\,°$C. The experimentally determined lattice mismatches with Si(111) are $+2\%$ for FeSi (CsCl) and -6.4% for ϵ-FeSi, respectively. We can rationalize these experimental findings as follows (see Fig. 1): Due to the large lattice mismatch, pseudomorphic ϵ-FeSi will have a very high
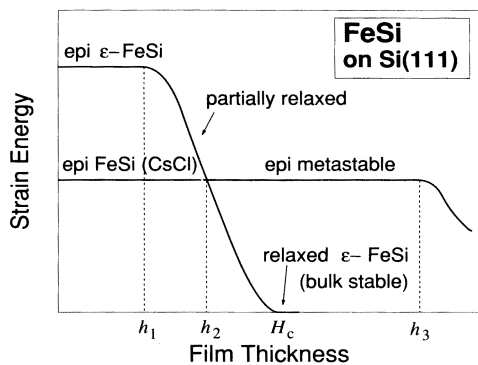
FIG. 1. Schematic diagram of epitaxial energy vs film thickness for FeSi on Si(111). The CsCl structure is more closely matched to the Si substrate than the bulk stable ϵ phase, and hence is epitaxially stable at small film thickness. Above its critical thickness H_c ϵ-FeSi is the most stable phase, and the occurrence of the CsCl phase in this range can be explained by the existence of a kinetic barrier. Upon annealing at $\sim 300\,^{\circ}$C the CsCl phase transforms irreversibly into the bulk ϵ phase.

strain energy, and a small critical thickness h_1, whereas the much smaller mismatch between FeSi (CsCl) and the Si substrate makes this material more stable at small thickness.[8] Since ϵ-FeSi is the stable bulk phase, however, above a critical thickness H_c where it is completely relaxed, it is lower in energy than the CsCl structure at any thickness. Therefore, at some thickness h_2 the two energy curves cross, and the CsCl structure ceases to be the epitaxially stable phase. From experiment we infer $h_2 \lesssim H_c \approx 15$ Å. Due to kinetic barriers (e.g., an energetically favorable interface structure), the CsCl phase is observed in metastable form even above h_2, and beyond its critical thickness $h_3 \approx 100$ Å up to ~ 1000 Å.

At composition ratio 1:2 the situation is less clear. Many epitaxial relations for β-FeSi$_2$/Si(111) with different lattice mismatches are reported,[10] and a disordered Fe$_{1-x}\square_x$Si phase of CsCl symmetry with an iron vacancy concentration $x = 0.5$ acts as a precursor to the ordered CaF$_2$ phase.[7,10] We will show, however, that the CaF$_2$ phase is even better lattice matched to Si than the CsCl phase, and hence a similar picture as sketched in Fig. 1 may apply also in this case.

Whereas the existence of epitaxial fluorite FeSi$_2$ is not that surprising in view of its relation to the bulk stable β phase and the existence of CoSi$_2$ and NiSi$_2$ in this crystal structure, the CsCl structure of FeSi seems to be rather "exotic." It is interesting to note that the only transition-metal silicides with composition MSi that occur in the CsCl structure are those with[11] M = Ru, Os, and Rh. Ruthenium and rhodium are the transition metals situated in the Pd row of the periodic table just below Fe and Co, respectively. These silicides normally order in the "FeSi" structure type, i.e., the structure of ϵ-FeSi, and only under certain growth conditions do they form the CsCl structure.[11] For instance, in the case of RuSi it was observed that the CsCl structure formed "more easily in mixtures that had not yet reached

equilibrium."[11] We have argued above that FeSi films are epitaxially metastable above ~ 15 Å, and only grow under the out-of-equilibrium conditions of low-temperature MBE. These considerations suggest that although the CsCl structure is extremely rare for monosilicides, it is nevertheless most likely to be formed by certain group-VIII transition metals, among which we find Fe and Co. Indeed, in Villars' three-dimensional structural stability diagram,[12] both compounds are found in regions of coexistence of the MnP-FeSi-CsCl structure types, but almost on the boundary with the region occupied by the CsCl structure. Very recently, epitaxial growth of CsCl-type CoSi on Si(111) has indeed been accomplished by MBE.[13] The existence of CsCl-type NiSi, however, seems less probable.

The great versatility of Fe to form a number of epitaxial silicides on Si—among which are found metals [FeSi(CsCl), γ-FeSi$_2$], semiconductors or semimetals (β-FeSi$_2$, ϵ-FeSi), and even magnetic compounds (Fe$_3$Si, possibly γ-FeSi$_2$)—offers a wide spectrum of potential applications. Theoretical studies of the electronic and structural properties of the Fe silicides are therefore of great interest. Semiconducting β-FeSi$_2$ has been studied by the linear muffin-tin orbital (LMTO),[4] and by the augmented spherical-wave[14] methods. In Ref. 4, the electronic structure of the fluorite phase γ-FeSi$_2$ is also given. The magnetic compound Fe$_3$Si (DO_3 structure) has been studied theoretically by Kudrnovský, Christensen, and Andersen.[15] We have recently published a brief account of the electronic band structure of FeSi in the CsCl structure, together with experimental results.[5]

In this work we concentrate on the properties of the bulk unstable "high-symmetry" compounds FeSi (CsCl structure) and γ-FeSi$_2$ (CaF$_2$ structure). We determine their lattice constants in order to better understand their existence as epitaxial phases on Si(111), and give a detailed account of their electronic band structures. We focus on the bonding between Fe and Si both in FeSi and γ-FeSi$_2$ and compare to NiSi$_2$ and CoSi$_2$. Special attention is given to the covalent versus ionic nature of the Fe-Si bond, and the role of Si p–Fe d interaction.

The paper is organized as follows. In Sec. II we present the details of our ab initio calculations and the resulting equilibrium structural parameters of the two hypothetical bulk phases; the Fe-Si bond is studied in Sec. III; in Sec. IV the electronic band structures are discussed; and finally the conclusions are given in Sec. V.

II. SELF-CONSISTENT CALCULATIONS

FeSi is assumed in the CsCl structure (space group $Pm\bar{3}m$), i.e., in a simple-cubic lattice with Fe at the origin and Si at the body center. Both types of atoms are coordinated with eight nearest neighbors (NN) of the other species. γ-FeSi$_2$ crystallizes in the CaF$_2$ structure (space group $Fm\bar{3}m$), i.e., in a face-centered-cubic lattice with Fe at the origin, and two Si atoms at positions $\pm(\frac{1}{4}\frac{1}{4}\frac{1}{4})$, respectively. Each Si atom is tetrahedrally coordinated with four metal atoms, and each metal atom has eight Si NN.

We have calculated the electronic energy eigenvalues, total energies, and wave functions of the two crystals with the self-consistent full-potential linearized augmented-plane-wave (FLAPW) method,[16] neglecting spin-polarization. The exchange-correlation energy is treated in the local-density approximation (LDA), using the Hedin-Lundqvist prescription. Wave functions are expanded in spherical harmonics with $l \leq 8$ ($l \leq 4$ for total energy minimization) inside the atomic spheres whose radii are 1.85 a.u. and 2.3 a.u. for Si and Fe, respectively. In the interstitial region a plane-wave basis is used with wave vectors up to 3.6 Ry (8.5 Ry) for wave functions (charge and potential). Integration in **k** space is approximated by summing over up to 48 **k** points in the irreducible wedge of the corresponding Brillouin zone. The energy-band structure and density of states (DOS) of the equilibrium structures are evaluated using higher cutoffs and more **k** points.

The lattice constants and bulk moduli obtained by total-energy calculations are summarized in Table I, together with the lattice constants of the bulk phases. We have fitted the total energies calculated at six different lattice constants to both Murnaghan's equation of state,[17] and a third- or fourth-order polynomial. The predicted equilibrium lattice constant is independent of the fitting procedure, whereas the fluctuations of the fitted bulk modulus provide the theoretical error bars given in Table I. The theoretical values predict a virtually perfect lattice match of CsCl-type FeSi and Si. Recent x-ray diffraction data[7] on thin epitaxial FeSi films yield a lattice constant $a_{FeSi}^{exp} = 2.77$ Å, which is 1.8% larger than our theoretical value, and a larger lattice mismatch with Si, i.e., $2a_{FeSi}^{exp} = 5.54$ Å ($a_{Si}^{exp} = 5.43$ Å), which remains, however, rather small. The predicted lattice constant of γ-FeSi$_2$ is only 2% smaller than that of FeSi (Table I), even though there are only half as many iron atoms per mole as in FeSi. Assuming the same magnitude of error on our predicted lattice constant as for the CsCl

structure, we obtain a corrected value of 5.42 Å, which is almost perfectly lattice matched with Si. This explains why the fluorite phase can compete with the lattice mismatched bulk phase (β-FeSi$_2$) in the presence of the Si substrate (see our discussion in Sec. I). While the Fe-Si NN distance differs by only 2% in the two crystals, the Fe-Fe NN distance is 2.72 Å in FeSi, and 3.76 Å in FeSi$_2$. Note that this Fe-Fe spacing in FeSi is only 10% greater than the NN distance, and 5% smaller than the next-nearest-neighbor distance along the cube edge in bcc iron.

Given the near lattice matching of both FeSi (CsCl) and FeSi$_2$ (CaF$_2$) with Si, we shall describe the electronic properties of the *unstrained* hypothetical equilibrium phases, rather than the rhombohedrally distorted ones observed on Si(111). The strain-induced changes on the electronic band structure are expected to be very small.

III. THE Fe-Si BOND

The nature of the chemical bond in transition-metal silicides has been the subject of extensive theoretical and experimental studies.[18-22] In general, the bonding in the silicides is understood in terms of metal d–silicon p hybridization. There has been a controversy about the bonding in NiSi$_2$. Tersoff and Hamann[19] proposed that the bonding in NiSi$_2$ and CoSi$_2$ is similar to that in Si, an idea first put forward by Chabal et al.[18] Following their arguments, the tetrahedrally coordinated Si atoms build sp^3 hybrids, which in the silicides form directed covalent bonding states with Fe d orbitals. In a later study, Lambrecht, Christensen, and Blöchl[21] came to a similar conclusion, but attributed more importance to the charge transfer from Si to Ni, which contributes an electrostatic term to the cohesive energy. It is well

TABLE I. Structural definition of the stable bulk phases[2] of FeSi and FeSi$_2$, as well as of the bulk unstable phases that exist epitaxially on Si(111). For the latter the theoretical predictions of the present work are compared to experimental values, where available, and to other theoretical results. The experimental lattice constant of Si is 5.43 Å.

Compound (Pearson symbol)	Space group	Lattice parameters (Å) (Expt.)	Lattice parameters (Å) (Theor.)	Bulk modulus (Mbar) (Theor.)
Bulk stable:				
ε-FeSi (cP8)	$P2_13$	$a = 4.46$		
β-FeSi$_2$ (oC48)	$Cmca$	$a = 9.86$ $b = 7.79$ $c = 7.83$		
Bulk unstable:				
FeSi (CsCl) (cP2)	$Pm\bar{3}m$	$2a = 5.54^a$	$2a = 5.44$	2.70 ± 0.07
Fe$_{1-x}\square_x$Si (CsCl, $x \leq 0.5$)	$Pm\bar{3}m$	$2a = 5.40^a$	($x = 0.5$)	
γ-FeSi$_2$ (CaF$_2$) (cF12)	$Fm\bar{3}m$		$a = 5.32$ $a = 5.39^b$	1.90 ± 0.05 2.06^b

^{a}Reference 7.
^{b}Reference 4.

TABLE II. Valence charge contained in the atomic spheres of radius R and in the interstitial volume of CsCl-type FeSi and CaF$_2$-type FeSi$_2$. The total valence charge of Fe is eight electrons, and that of Si is four electrons.

	Charge	Fe $R = 2.3$ a.u.	Si $R = 1.85$ a.u.	Interstitial	Total
Fe, Si	isolated atoms	6.24	1.25		
FeSi	free-atom superposition	7.30	1.66	3.04	12.0
	self-consistent	7.48	1.48	3.04	12.0
FeSi$_2$	free-atom superposition	7.22	1.55	5.68	16.0
	self-consistent	7.57	1.42	5.59	16.0

known, however, that the charge transfer is not uniquely determined, since it depends on the choice of the "atomic spheres" where the charge is measured. With this in mind, we compare in Table II the valence charge contained in the atomic spheres used in our calculations. Besides the self-consistent density of the two crystals we have calculated the charge density of the isolated atoms as well as the lattice superpositions of the atomic densities. In FeSi$_2$, the eight Si NN of Fe contribute more charge to the Fe spheres due to the smaller Fe-Si distance. On the other hand, the six Fe NN of Fe in FeSi are much closer than the 12 Fe NN of Fe in FeSi$_2$, therefore superposition of atomic densities gives a Fe charge 0.08 electrons *larger* in FeSi than in FeSi$_2$. As to the charge in the Si spheres, it is obvious that twice the number of Fe NN of Si in FeSi yields a larger overlap than the corresponding one in FeSi$_2$. The remaining free-atom charge is distributed in the interstitial region. When comparing the free-atom superpositions with the self-consistent densities, we observe an additional *net* charge transfer ΔQ_{Fe} of 0.18 electrons into the Fe sphere in FeSi, and one of 0.35 electrons into the Fe sphere in FeSi$_2$. Note that now the Fe sphere in FeSi$_2$ contains more charge than the one in FeSi. It would be misleading, however, to draw conclusions on the ionicity from these numbers alone, due to the ambiguity pointed out above. We will show that the excess charge in the FeSi$_2$ Fe sphere with respect to the

FeSi one is due to a piling up of covalent charge in the Fe-Si bond region of FeSi$_2$.

Toward this end we analyze the charge *densities* instead of the integrated charge in the spheres. In Fig. 2 we display contour plots of the difference between the self-consistent charge density and the superposition of atomic densities in the (110) plane of FeSi$_2$ (a) and FeSi (b). Besides the obvious difference due to the presence of an additional Fe atom in FeSi, we notice a weak piling up of charge midway between Fe and Si in the fluorite structure. This covalent charge accumulation is almost entirely contained in the Fe sphere, and is responsible for the larger charge transfer in FeSi$_2$ discussed above. In FeSi, on the other hand, the charge redistribution is unimportant in the interstitial and bond region, and we interpret the charge transfer of 0.18 electrons from the Si to the Fe spheres as a real ionic character of the bond. This conclusion will be reinforced by the crystal-field arguments presented in Sec. IV.

IV. ELECTRONIC STRUCTURE

The energy dispersion relations of γ-FeSi$_2$ and CsCl-type FeSi can be found in Refs. 4 and 5, respectively, and are not reproduced here. In Fig. 3 we show the DOS of the two materials instead.[23] In Table III we provide the angular-momentum projected densities at E_F and inte-

$\Delta Q_{Fe} = 0.35e \quad \Delta Q_{Si} = -0.13e \qquad \Delta Q_{Fe} = 0.18e \quad \Delta Q_{Si} = -0.18e$
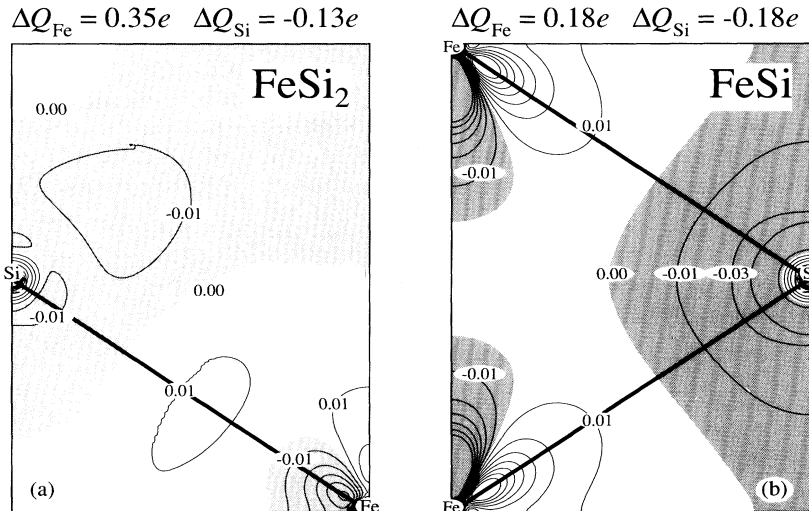

FIG. 2. Contour plot of the difference between the self-consistent charge density and the superposition of atomic densities in the (110) plane of CaF$_2$-type FeSi$_2$ (a) and CsCl-type FeSi (b). Areas of negative values are shaded, contours are labeled in units of 10^{-2} electrons/(bohr)^3, and the level spacing is 0.02 in these units. ΔQ_{α} is the difference between the self-consistent valence charge and the superposition of the atomic valence charges in the sphere centered on atom α. The Fe-Si bonds are indicated with solid lines.
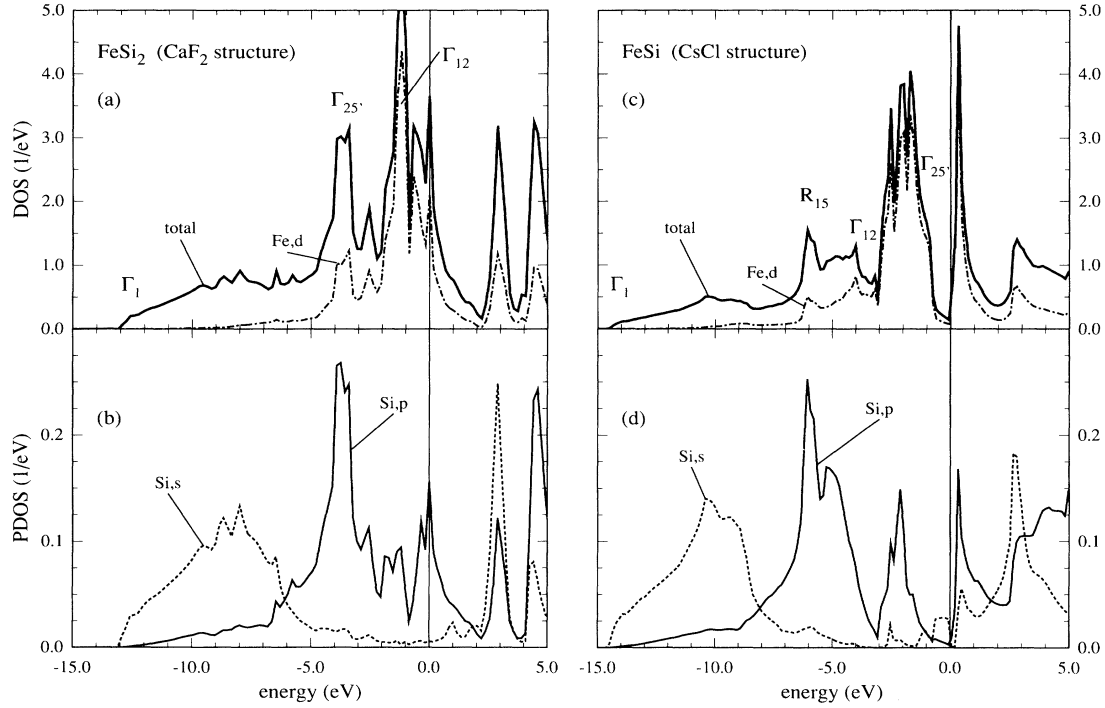
FIG. 3. DOS of CaF_2-type $FeSi_2$ (left panel) and CsCl-type FeSi (right panel). (a) and (c) show the total (solid line) and partial Fe d (dashed-dotted line) DOS in eV^{-1} per unit cell, (b) and (d) show the partial Si p (solid line) and Si s (dashed line) DOS. The partial DOS are projected on *one* atomic sphere in both structures. The energy is measured relative to the Fermi level (indicated by a solid vertical line).

grated up to E_F, respectively. Our DOS for $FeSi_2$ is in perfect agreement with the LMTO one by Christensen.[4] The two main peaks in the valence spectrum originate from the metal d–Si p bonding states at ~ -4 eV ($\Gamma_{25'}^v$ states at the zone center) and from the nonbonding metal d-band manifold centered at ~ -1.5 eV (Γ_{12}^v states at the zone center), respectively. LDA energy eigenvalues at high-symmetry points are listed in Table IV, together with the angular-momentum decomposition of the wave functions inside the atomic spheres. The pd hybridization broadens the metal d bands considerably as can be seen from the DOS and the orbital characters of the eigenfunctions. Given the strong similarity between the present Si s and p partial DOS with those of $CoSi_2$,[19] we conclude that the binding mechanism in $FeSi_2$ is basically the same as in the former compound. It has been shown by Christensen that the rigid-band assumption is nearly fulfilled for the three compounds $FeSi_2$, $CoSi_2$, and $NiSi_2$ (see

Fig. 1 in Ref. 4), and therefore the number of valence electrons pins the position of the Fermi level in an otherwise similar DOS. At the Fermi level there is a rather strong peak in the d DOS of $FeSi_2$ (28.5 Ry^{-1}, cf. Table III), with an appreciable admixture of Si p states. The location in **k** space of these states is shown in Ref. 4 to be on the hexagonal Brillouin-zone face. We have previously estimated[6] that the Stoner factor is considerably larger than unity and explained bulk instability of the fluorite phase in terms of the Stoner model. Indeed, a spin-polarized calculation by Christensen predicts a ferromagnetic moment of 0.3 μ_B per formula unit.[4] Experimental confirmation of ferromagnetism in γ-$FeSi_2$ is still lacking, since the grown films are very thin (≤ 15 Å) and magnetic measurements are difficult to perform. Above E_F we observe a Si sp antibonding peak at 3 eV, which seems to be even more pronounced than in $CoSi_2$,[19] and which is a typical fingerprint of sp^3 hybridization. To-

TABLE III. Partial number of states (NOS) below the Fermi energy E_F, and density of states at E_F (DOS in Ry^{-1}) normalized to one atomic sphere (cf. Table II) in CsCl-type FeSi and CaF_2-type $FeSi_2$.

		Fe s	Fe p	Fe d	Si s	Si p	Si d
FeSi	DOS	0.001	0.018	1.678	0.051	0.020	0.004
	NOS	0.385	0.530	6.528	0.599	0.720	0.143
$FeSi_2$	DOS	0.317	3.740	28.478	0.073	2.115	0.449
	NOS	0.466	0.540	6.544	0.607	0.706	0.099

TABLE IV. FLAPW energy eigenvalues at high-symmetry points of the face-centered-cubic Brillouin zone for $FeSi_2$ in the CaF_2 structure. Energies are measured relative to the Fermi level. The probability of the orbital character of the wave functions inside the Fe and Si atomic spheres is given in percent. In the last column we list the probability in the interstitial region.

State	Energy (eV)	Fe			Si			Int.
		s	p	d	s	p	d	
Γ_1^v	-13.07	14			30			56
$\Gamma_{25'}^v$	-3.95			50		17		32
Γ_{12}^v	-1.40			80			3	17
$\Gamma_{2'}^c$	0.87				67			29
Γ_{15}^c	3.85		28			2	13	56
$X_{1'}^v$	-8.93		10		36		1	52
X_1^v	-7.09	15		8		19		58
X_3^v	-6.43			28	33		2	37
X_5^v	-3.49		13			27		59
X_1^v	-1.44	14		52		1	5	28
X_5^v	-1.43			86		4	1	9
X_2^v	-0.67			91				8
X_1^c	2.60			74	16			10
L_1^v	-9.73	13		5	26	5		51
$L_{2'}^v$	-9.16		10		26	6		58
L_3^v	-3.41			53		13	1	32
L_1^v	-1.70	9		63	2	5	2	17
L_3^v	-1.04			87			1	11
$L_{3'}^v$	-0.24		16			26	4	53
$L_{2'}^c$	2.74				23	11	3	59

gether with the discussion of the charge transfer in Sec. III the picture of covalent bonding in fluorite $FeSi_2$ is thus confirmed, similarly to the case of $CoSi_2$ and $NiSi_2$, and in agreement with the interpretation of Tersoff and Hamann[19] for the latter two compounds. In $FeSi_2$, however, the covalent contribution to the free energy is too small to stabilize the fluorite phase in bulk form. The kinetics and epitaxial constraints of iron silicide grown by MBE on Si(111), however, lead to the formation of fluorite $FeSi_2$ as an intermediate step of the disordered

$Fe_{0.5}\square_{0.5}Si$ to β-$FeSi_2$ transition[5,7] at $\sim 500°C$.

Let us now turn to FeSi (right panel in Fig. 3, and Table V). Again the total DOS is dominated by the metal d bands, giving rise to a strong 2-eV broad peak centered at ~ -2 eV. The Fermi level is located at the upper end of a region of low DOS, at the onset of a less pronounced, sharp peak of Fe d states. The valence DOS agrees very well with the ultraviolet photoemission spectrum of Ref. 5, provided that the theoretical curve is shifted by ~ 1 eV towards E_F. This final-state effect is discussed in

TABLE V. FLAPW energy eigenvalues at high-symmetry points of the simple-cubic Brillouin zone for FeSi in the CsCl structure. Energies are measured relative to the Fermi level. The probability of the orbital character of the wave functions inside the Fe and Si atomic spheres is given in percent. In the last column we list the probability in the interstitial region.

State	Energy (eV)	Fe			Si			Int.
		s	p	d	s	p	d	
Γ_1^v	-14.60	24			27			48
Γ_{12}^v	-4.12			76			3	20
$\Gamma_{25'}^v$	-0.88			95			1	3
Γ_{15}^c	3.38		17			37		40
R_{15}^v	-6.30			50		16		34
$R_{1'}^v$	-1.27				64			30
R_{12}^c	0.07			99				1
R_{15}^c	1.67		39				12	48
$X_{2'}^v$	-10.47		17		34			48
X_1^v	-9.04	26		10		17		46
X_3^v	-3.15			87				12
X_5^v	-2.53			81		6		11
X_4^v	-0.69			97				2
X_3^c	0.34	4		89		2		4

more detail in Ref. 5. A very similar DOS is also predicted for CsCl-type RuSi by a LMTO Green's function calculation of Ivanovskii.[24] There it is also shown that RhSi has a virtually identical DOS, except for the position of E_F, which now falls at higher energy in the sharp d peak. The same behavior can therefore be anticipated when replacing Fe by Co in FeSi, indicating that the hypothetical CsCl phase of CoSi is even less stable than FeSi, and likely to be magnetic. Below E_F the Si s and p projected DOS is rather similar to that in $FeSi_2$. This does not imply the formation of sp^3 hybrids, however, since Si is now eightfold coordinated, instead of fourfold as in the fluorite structure. We attribute the relatively large width of the Si s band to bonding with Fe s and p states (see Table V).

An important difference between the band structures of the two materials lies in the order of the Fe d bands at Γ: in FeSi $\Gamma_{25'}$ lies above Γ_{12}, whereas in $FeSi_2$ $\Gamma_{25'}$ lies below Γ_{12}. An inverted crystal-field splitting was previously noted in band calculations of chalcopyrites[25] ($CuInSe_2$) and in II-VI compounds.[26] The results were explained in terms of symmetry-enforced pd couplings. A similar interpretation is pertinent here: In FeSi the Si p bands (x, y, z) transform like Γ_{15}, and thus do not mix with the d-band triplet (xy, yz, zx) of Fe, which transforms like $\Gamma_{25'}$. Hence, the crystal-field splitting corresponds to Γ_{12} below $\Gamma_{25'}$ as predicted by the point-ion model. This mixing is allowed, however, in the fluorite structure, where the p orbitals of the two Si atoms in the unit cell originate both Γ_{15} and $\Gamma_{25'}$ states. The resulting pd bonding lowers the $\Gamma_{25'}$ level relative to the nonbonding Γ_{12} level, thus reversing the sign with respect to that originating from the crystal-field splitting alone. This effect is illustrated in Fig. 4, where the energy levels of the Fe d and Si p states are shown for $FeSi_2$ in the CaF_2 structure, (a) without and (b) with taking the pd inter-

FIG. 4. Energy levels of Fe d and Si p bands at Γ in the CaF_2 structure of $FeSi_2$, (a) neglecting, (b) including Fe d–Si p interaction. Note that pd repulsion pushes the $\Gamma_{25'}$ states below the Γ_{12} states, whereas crystal-field splitting alone (a) predicts the Γ_{12} states to be lowest.

action into account. The pd repulsion found in certain II-VI zincblende semiconductors has a similar origin:[26] the cation d bands of Γ_{15} symmetry mix with the anion p bands and are pushed below the Γ_{12} d states, opposed to crystal-field considerations alone. Note, however, that the pd repulsion in ZnTe, CdTe, and HgTe, e.g., is much weaker than in the present case of $FeSi_2$ and in the case of the chalcopyrites, since (i) the cation d–anion p energy separation is larger for these atom pairs than for Fe and Si, and (ii) the cation-anion distance is considerably larger than the Fe-Si one in $FeSi_2$. Therefore, the Γ_{15}-Γ_{12} splittings are much smaller in magnitude in these II-VI compounds[26] than the $\Gamma_{25'}$-Γ_{12} splitting in $FeSi_2$, which we predict to be -2.55 eV.

In FeSi, on the other hand, $E(\Gamma_{25'}) - E(\Gamma_{12}) = +3.24$ eV, which is an unusually large crystal-field splitting. We argue that it has two major contributions, an ionic one and one due to repulsion between Fe d states of neighboring Fe atoms. Placing positive point charges $+ze$ on the Si atom sites and negative charges $-ze$ on the Fe sites will lower the electrostatic binding energy of the Γ_{12} states relative to the $\Gamma_{25'}$ ones. We estimate the ionic contribution ΔE_i to the splitting by assuming analytic Slater orbitals for the Fe $3d$ wave functions, and by performing the lattice sum involved in the fourth-order nonspherical portion of the crystal potential as described by Callaway[27] for cubic crystals. We obtain $\Delta E_i \approx +1.14z$ eV for $Fe^{-z}Si^{+z}$. Clearly, this crude point-charge ionic model is not sufficient to quantitatively explain the level splitting, but the important points are that the sign agrees with the calculated one and that ionicity contributes to the splitting. A similar calculation for the fluorite structure (placing the charge $-2ze$ on the Fe sites) yields a d-level splitting with *equal* sign as in FeSi, but 40% smaller. This is not surprising, since the nearest-neighbor configuration of the Fe atoms is the same for both structures, and the contribution from the outer shells decreases rapidly.[27] Hence, neglecting p-d bonding in the fluorite structure the Γ_{12} states would be *lower* in energy than the $\Gamma_{25'}$ ones [Fig. 4(a)], very much like in the CsCl structure. This shows once more that ionicity is not important in $FeSi_2$.

The other effect that contributes to the large splitting in FeSi is the Fe-Fe interaction. We noted in Sec. II that the Fe-Fe NN distance in FeSi is rather close to the equilibrium bond length in bcc iron. According to Harrison[28] the dd interatomic matrix elements decrease with the fifth power of the distance, and should therefore be about 60% as large as in bcc iron. Recent tight-binding fits to the present band structures show indeed that the Fe-Fe dd interaction cannot be neglected in FeSi, whereas it is less important in[29] $FeSi_2$. In FeSi the Fe atoms occupy simple-cubic lattice points, and hence are octahedrally coordinated to their nearest Fe neighbors. The Γ_{12} orbitals form σ bonds, whereas the $\Gamma_{25'}$ orbitals are π bonded. Using Harrison's universal tight-binding parameters[28] a splitting of ~ 2.2 eV is obtained. Again, this is not sufficient by itself to explain the splitting obtained in the self-consistent calculation. Considering in addition the ionic contribution discussed above, however, (calculated with a better approximation than the point-
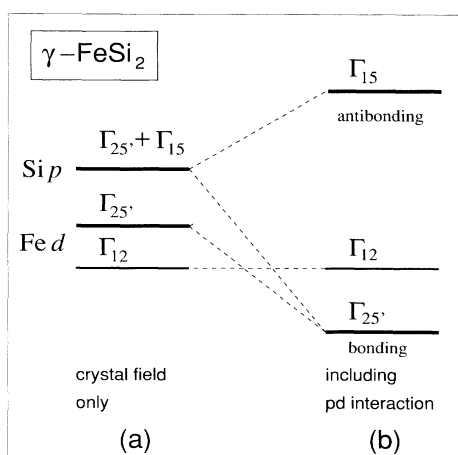
charge model) one should recover the $\Gamma_{25'}$-Γ_{12} splitting of the FLAPW calculation.

Inspection of Table V and of Fig. 3 (right panel) shows that Si p–Fe d hybridization is present also in FeSi, although to a smaller extent than in FeSi$_2$, at **k** points other than Γ. At the R point, e.g., the **k**-dependent phase factors associated with the atomic orbitals in a linear-combination-of-atomic-orbitals (LCAO) scheme cause the Si (x, y, z)-like and the Fe (xy, yz, zx)-like wave functions to belong to the same irreducible representation R_{15}, as they do under the T_d point group. Also along the Λ line pd hybridization is allowed by symmetry, and leads to anticrossing (see Fig. 4 in Ref. 5) of the twofold degenerate Λ_3 bands originating from both Γ_{12} and $\Gamma_{25'}$ (retaining only dd matrix elements, these bands would cross along Λ). Due to pd bonding the R_{15} state is pushed below Γ_{12}, and contributes to the peak in the DOS at ~ -6 eV (see Fig. 3). The upper Λ_3 band ends in a "dd-antibonding" R_{12}^c state close to the Fermi level, with 99% d character in the Fe atomic spheres. Due to the strong dd interaction we refrain from using the term "nonbonding d" for these states.

V. CONCLUSIONS

We have presented a theoretical study of the electronic and structural properties of the bulk unstable cubic iron silicide FeSi(CsCl), and have compared them with those of γ-FeSi$_2$(CaF$_2$). Both structures exist epitaxially on Si(111) due to a lattice mismatch with Si which is smaller than that of the bulk stable phases ϵ-FeSi and β-FeSi$_2$, respectively. In addition, kinetic barriers are believed to exist which account for the observed metastability of FeSi (CsCl) films at thicknesses exceeding its epitaxial stability range (Fig. 1).

We have established the close resemblance of the bonding configuration of FeSi$_2$ with CoSi$_2$ and NiSi$_2$, i.e., Si sp^3 hybridization, strong metal d-Si p bonding, the presence of directed covalent Fe-Si bonds, and negligible ionicity. The giant density of d states at the Fermi level leads to a Jahn-Teller instability of the bulk compound, explaining its absence in the bulk phase diagram.

CsCl-type FeSi, on the other hand, is characterized by a small charge transfer from Si to Fe, strong Fe-Fe dd bonding, and to some extent also by Si p-metal d interaction. We have shown that both the charge distribution and the electronic band structure of the two materials are

consistent with the bonding mechanisms presented in this work. An empirical tight-binding study of the Fe silicides is underway,[29] and will address the lattice dynamics and its implications on the $\gamma \to \beta$ phase transition in epitaxial FeSi$_2$-Si(111).

Comparison with other known monosilicides in the CsCl structure has allowed us to speculate on the possible existence of epitaxial CoSi(CsCl) on Si(111). Subsequent experiments have confirmed the epitaxial stability of this phase. A rigid-band model implies a rather high d DOS at the Fermi level, which may cause the compound to order magnetically.

The disordered CsCl phase Fe$_{1-x}\square_x$Si is observed over a wide range of Fe vacancy concentrations $0 < x \leq 0.5$. From the present study of the ordered end compounds FeSi and FeSi$_2$ we presume that the ionic, or Madelung contribution to the cohesive energy (present in the CsCl, but not in the CaF$_2$ phase) stabilizes the epitaxial disordered Fe$_{0.5}\square_{0.5}$Si CsCl structure relative to the ordered CaF$_2$ structure. In the latter the Fe atoms are located on alternate $\{111\}$ planes, and the Si atoms are tetrahedrally coordinated with the Fe atoms. The role of the d electrons, however, cannot be obtained from the properties of the end compounds alone. A rigid-band model would predict the Fermi level to fall in a region of high d DOS for increasing x, which is hardly reconciled with the experimentally observed epitaxial stability and absence of magnetic order in the defect CsCl phase. Further theoretical studies using, e.g., the coherent phase approximation, are needed for a complete understanding of the electronic properties of Fe$_{1-x}\square_x$Si as a function of x. We hope that the present study, which adds to the general understanding of transition-metal silicides, will stimulate further theoretical and experimental work on the fascinating iron silicide system.

ACKNOWLEDGMENTS

* Also at Institut de Physique Appliquée, Ecole Polytechnique Fédérale, Lausanne, Switzerland. Present address: National Renewable Energy Laboratory, 1617 Cole Boulevard, Golden, CO 80401-3393.

† Also at Department of Theoretical Physics and INFM, University of Trieste, I-34014 Trieste, Italy.

[1] H. von Känel, Mater. Sci. Rep. **8**, 193 (1992).

[2] *Atlas of Crystal Structure Types for Intermetallic Phases*, edited by J. L. C. Daams, P. Villars, and J. H. N. van Vucht (American Society for Metals International, Materi-

als Park, OH, 1991).

[3] *Binary Alloy Phase Diagrams*, edited by T. B. Massalski (American Society for Metals International, Materials Park, OH, 1986), Vol. 2, p. 1108.

[4] N. E. Christensen, Phys. Rev. B **42**, 7148 (1990).

[5] H. von Känel, K. A. Mäder, E. Müller, N. Onda, and H. Sirringhaus, Phys. Rev. B **45**, 13807 (1992).

[6] N. Onda, J. Henz, E. Müller, K. A. Mäder, and H. von Känel, Appl. Surf. Sci. **56-58**, 421 (1992); N. Onda, J. Henz, E. Müller, H. von Känel, C. Schwarz, and

R. E. Pixley, Helv. Phys. Acta **64**, 197 (1991); H. von Känel, R. Stalder, H. Sirringhaus, N. Onda, and J. Henz, Appl. Surf. Sci. **53**, 196 (1991).

[7] N. Onda, H. Sirringhaus, S. Goncalves-Conto, C. Schwarz, E. Müller-Gubler, and H. von Känel, Mater. Res. Soc. Symp. Proc. (to be published).

[8] D. M. Wood and A. Zunger, Phys. Rev. B **40**, 4062 (1989); A. Zunger and D. M. Wood, J. Cryst. Growth **98**, 1 (1989).

[9] R. Bruinsma and A. Zangwill, J. Phys. (Paris) **47**, 2055 (1986).

[10] H. Sirringhaus, N. Onda, E. Müller-Gubler, P. Müller, R. Stalder, and H. von Känel, Phys. Rev. B **47**, 10 567 (1993).

[11] L. N. Finnie, J. Less-Common Met. **4**, 24 (1962).

[12] P. Villars, J. Less-Common Met. **92**, 215 (1983).

[13] C. Schwarz, S. Goncalves-Conto, H. Sirringhaus, and H. von Känel (unpublished).

[14] R. Eppenga, J. Appl. Phys. **68**, 3027 (1990).

[15] J. Kudrnovský, N. E. Christensen, and O. K. Andersen, Phys. Rev. B **43**, 5924 (1991).

[16] H. Jansen and A. J. Freeman, Phys. Rev. B **30**, 561 (1984).

[17] F. D. Murnaghan, Proc. Natl. Acad. Sci. USA **30**, 244 (1944).

[18] Y. J. Chabal, D. R. Hamann, J. E. Rowe, and M. Schlüter, Phys. Rev. B **25**, 7598 (1982).

[19] J. Tersoff and D. R. Hamann, Phys. Rev. B **28**, 1168 (1983).

[20] O. Bisi and C. Calandra, J. Phys. C **14**, 5479 (1981).

[21] W. R. L. Lambrecht, N. E. Christensen, and P. Blöchl, Phys. Rev. B **36**, 2493 (1987).

[22] J. H. Weaver, A. Franciosi, and V. L. Moruzzi, Phys. Rev. B **29**, 3293 (1984).

[23] Note that the DOS presented here is based on the LDA. Self-energy corrections are known to shift energy eigenvalues below E_F to lower energies in proportion to the degree of their spatial localization. Thus, d states will move more than sp states. These corrections should not affect our conclusions, however.

[24] A. L. Ivanovskii, Izv. Akad. Nauk SSSR, Neorg. Mater. **26**, 1226 (1990) [English translation: *Inorganic Materials* (Plenum, New York, 1990)].

[25] J. E. Jaffe and A. Zunger, Phys. Rev. B **28**, 5822 (1983).

[26] S.-H. Wei and A. Zunger, Phys. Rev. B **37**, 8958 (1988).

[27] J. Callaway, *Quantum Theory of the Solid State*, 2nd ed. (Academic, Boston, 1991), p. 221.

[28] W. A. Harrison, *Electronic Structure and the Properties of Solids* (Freeman, San Francisco, 1980).

[29] G. Malegori and L. Miglio (private communication).

$\Delta Q_{Fe} = 0.35e$ $\Delta Q_{Si} = -0.13e$
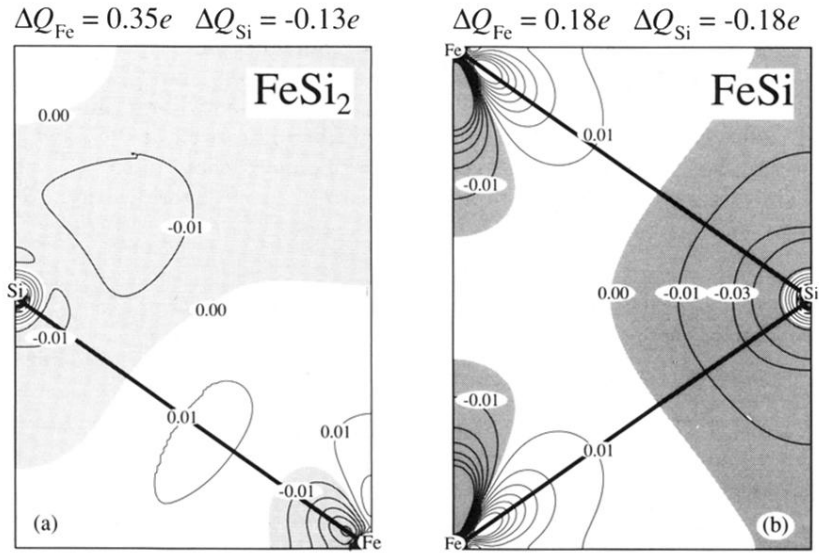
$\Delta Q_{Fe} = 0.18e$ $\Delta Q_{Si} = -0.18e$

FIG. 2. Contour plot of the difference between the self-consistent charge density and the superposition of atomic densities in the (110) plane of CaF_2-type $FeSi_2$ (a) and CsCl-type FeSi (b). Areas of negative values are shaded, contours are labeled in units of 10^{-2} electrons/(bohr)^3, and the level spacing is 0.02 in these units. ΔQ_α is the difference between the self-consistent valence charge and the superposition of the atomic valence charges in the sphere centered on atom α. The Fe-Si bonds are indicated with solid lines.